Electronic Supporting Information

Near-Infrared Selective Dynamic Windows controlled by Charge Transfer Impedance at Counter Electrode

*P. Pattathil, R. Scarfiello, R. Giannuzzi, G. Veramonti, T. Sibillano, A. Qualtieri, C. Giannini, P. D. Cozzoli and M. Manca**

*corresponding author e-mail: michele.manca@iit.it

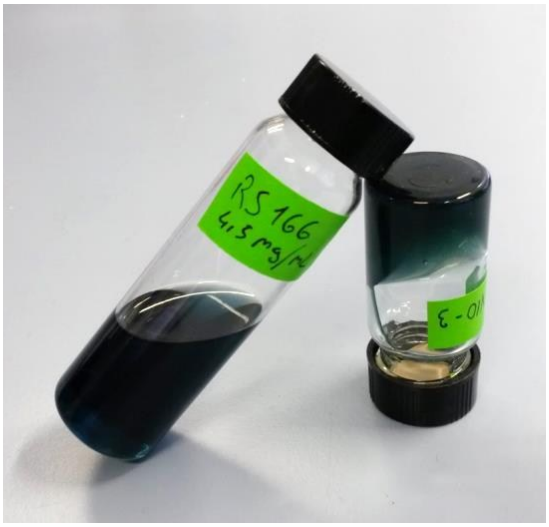

Figure S1. Daylight pictures of (left vial) a colloidal solution batch of as-synthesized $W_{18}O_{49}$ NRs and of (right vial) a corresponding $W_{18}O_{49}$ NR-based viscous paste used to prepare the EC devices.

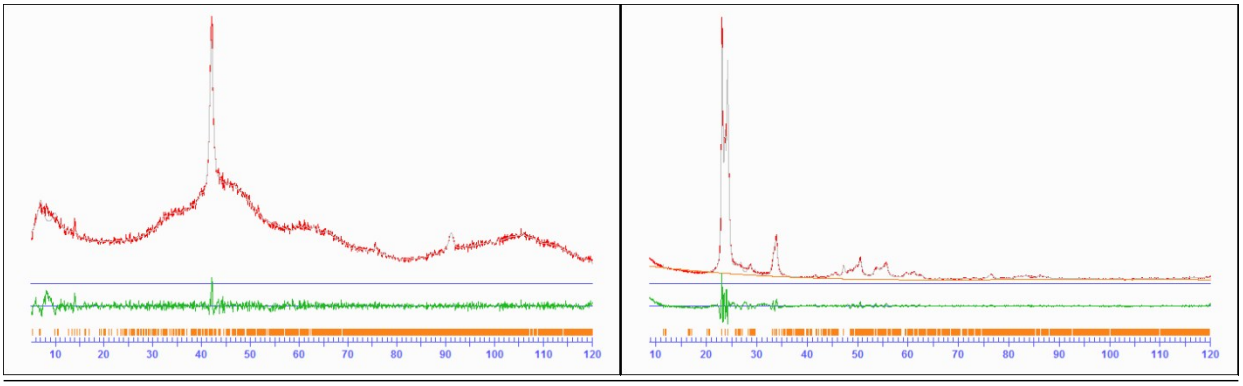

Figure S2. Indexing of XRD data (red curves) to the monoclinic phase of bulk $W_{18}O_{49}$ (ICSD code #15254) (left panel) and to the triclinic WO_3 phase (ICSD #80055) (right panel) performed by means of Rietveld fits (grey curves)

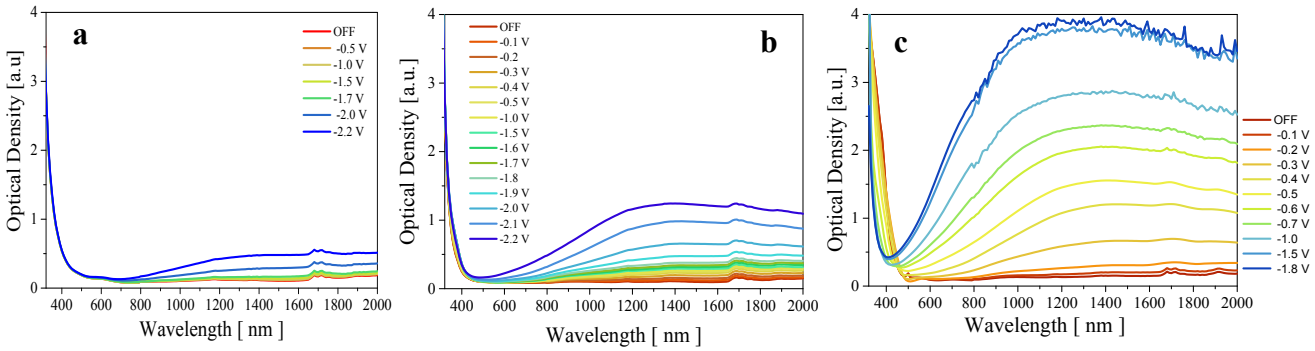

Figure S3. Modulation of the optical density detected on WO_3-NR-based EC cells filled with the three different ELs, namely: a) EL#1, b) EL#2, c) #EL3.

A set of **cyclic voltammetry measurements** was carried out on a 500 nm-thick WO_3-NR electrode (deposited on ITO and thermally sintered at 400°C in air) by using a three-electrode setup connected to a potentiostat/galvanostat (PGSTAT 302N Autolab, Eco-Chemie, The Netherlands). The counter electrode was a Pt foil. The reference electrode was an Ag/AgCl wire in saturated LiCl (Merck) dissolved in anhydrous propylene carbonate. The potential of this electrode was −0.05 V versus Ag/AgCl. The measured potentials were referenced to the Ag/AgCl electrode. Analysis of the voltammetric sweep rate dependence enabled us to decouple quantitatively the capacitive contribution to the current response. The current response at a fixed potential can be expressed as arising from the combinedcontributions of two independent mechanisms, namely surface capacitive effects and diffusion-controlled Li insertion processes. [Wang et al. *J. Phys. Chem.* C 2007, 111, 14925– 14931]:

$$i(V) = k_1 v + k_2 v^{1/2}$$

We estimated that, at a scan rate of 2mV/s, the contribution arising from double-layer surface capacitance approaches 25% of the total amount of accumulated charges.

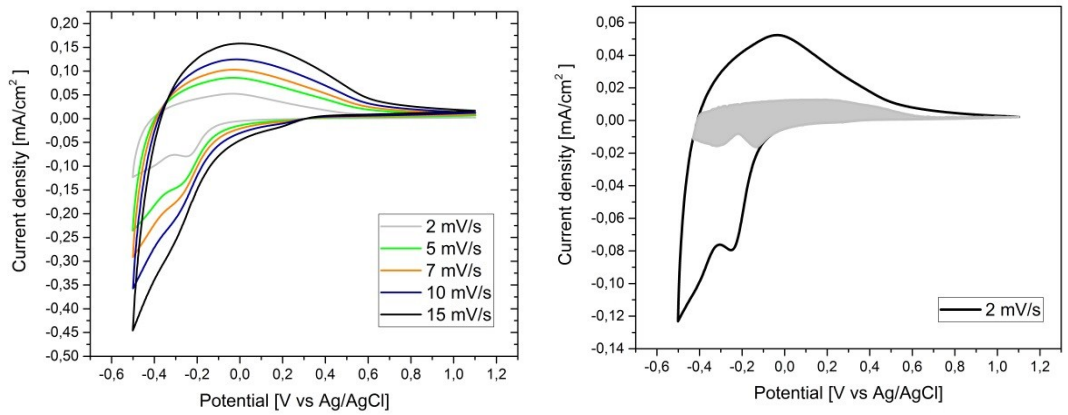

Figure S4. a) Cyclic voltammetry plots of a WO_3-NRs electrode measured at various scan rates (ranging from 2 to 15 mV/s); b) Estimation of the contribution due to surface capacitance (identified by shaded area) in the CV plot measured at a scan rate of 2 mV/s.

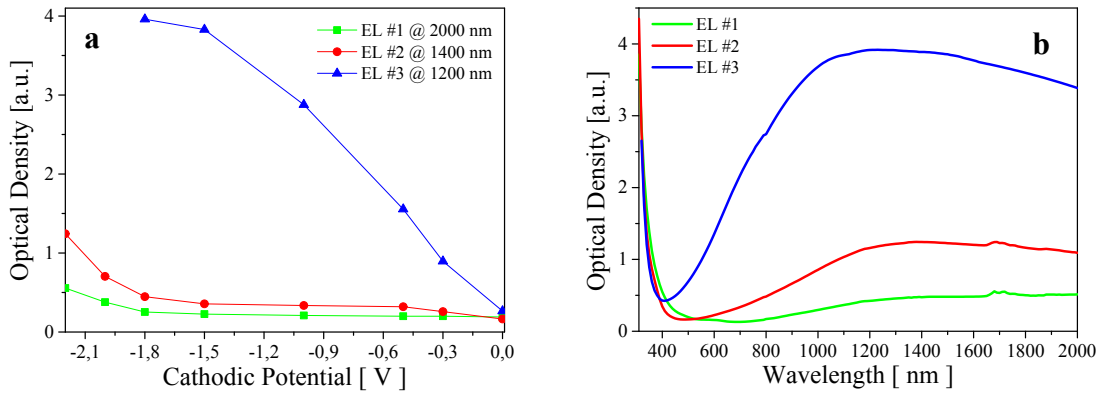

Figure S5. a) Variation of the optical density of WO_3-NR-based EC cells filled with three different ELs as a function of the applied bias potential values; b) Optical density of the same cells detected upon the application of highest voltage, namely -2.2 V for EL #1 and EL #2, and -1.8 V for EL #3, respectively.

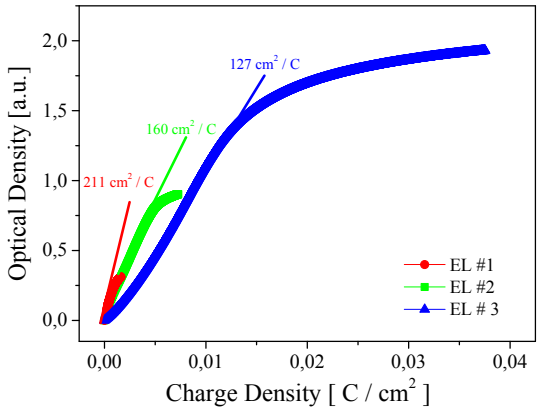

Figure S6. Variation of the optical density at 1500 nm as function of the injected charge density into WO_3-NR-based EC cells filled with the three different ELs.

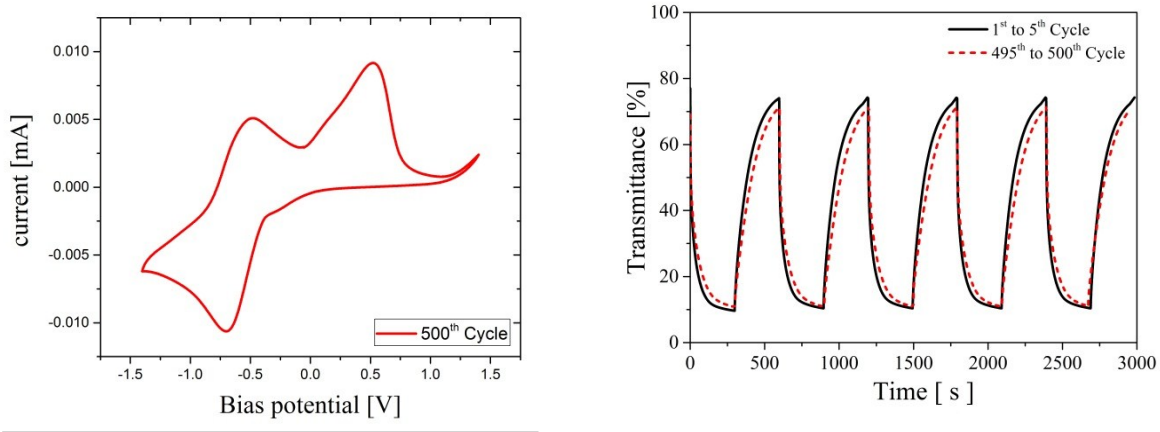

Figure S7. a) Cyclic voltammetry plots of a WO_3-NRs electrode filled with EL #2 measured after 500 scan b) Variation of the optical transmittance at 1500 nm of the WO_3-NR based EC cells filled with EL #2